electronics

MDPI

Article

Joint Analysis of Front-Door and Back-Door Couplings of PIN Limiter Based on Improved Equivalent Circuit Model

Tao Liu [1], Le Xu [1,*], Qiwei Li [2], Bin Yao [1] and Xiaowei Shi [1]

[1] School of Electronic Engineering, Xidian University, Xi'an 710071, China
[2] China Academy of Space Technology, Xi'an 710129, China
* Correspondence: lexu@mail.xidian.edu.cn

Abstract: Based on the previous research on electromagnetic pulse coupling, which pays more attention to the front-door coupling or the back-door coupling alone, this paper analyzes the influence of an electromagnetic pulse on electronic devices and systems through the joint analysis of front-door and back-door couplings using the finite-difference time-domain method (FDTD). This specific measure is used to simplify the front-door coupling to the voltage source injection, which occurs simultaneously with plane wave irradiation. This coupling scheme of the front door and back door with the voltage source and plane wave acting simultaneously is rarely seen in previous analyses, which also gives consideration to the working state of the circuit. Although the equivalent circuit model is widely used, it cannot effectively reflect the working state of the diode circuit under the conditions of large injection and high frequency. In view of the limited application scenarios of the traditional equivalent circuit model, which cannot accurately describe the internal response characteristics of the diode under different electromagnetic pulse coupling, this paper introduces an improved equivalent circuit model based on the physical model. Taking the Positive Intrinsic-Negative (PIN) limiter as the target, this paper analyzes the influence of the front-door and back-door joint coupling on its performance under different electromagnetic pulses and then gives protection suggestions.

Keywords: equivalent circuit model; physical model; limiter; diode; electromagnetic coupling; FDTD; field-circuit coupling

Citation: Liu, T.; Xu, L.; Li, Q.; Yao, B.; Shi, X. Joint Analysis of Front-Door and Back-Door Couplings of PIN Limiter Based on Improved Equivalent Circuit Model. *Electronics* **2022**, *11*, 3921. https://doi.org/10.3390/electronics11233921

Academic Editor: Anna Richelli

Received: 26 October 2022
Accepted: 24 November 2022
Published: 28 November 2022

1. Introduction

With the development of high-precision integrated circuits and the rapid development of electronic science and technology, the components of electronic equipment are becoming more intensive [1], the working frequency of the equipment is gradually rising, and the required power consumption is gradually declining. At the same time, many hidden dangers are becoming obvious [2,3], such as the increasingly complex electromagnetic environment and the higher electromagnetic sensitivity of communication equipment to the outside world.

The way in which electromagnetic pulse affects electronic equipment is mainly divided into front-door coupling and back-door coupling [4–6]. Front-door coupling enters the device through an antenna. Back-door coupling refers to the coupling of the electromagnetic pulse into the equipment by cables connected between different devices or slots in the system.

A large number of scholars have conducted research on the coupling effect of electromagnetic pulses on electronic systems [7,8]. Frank Sabath set up a short pulse simulator for susceptibility investigations, which consists of a compact ultrawide-band source and a half-impulse radiating antenna [9]. For the front-door coupling, the antenna is modeled by different full-wave numerical methods. Simulation usually consumes a lot of computing time and memory because the antenna needs a more refined grid to simulate its

electromagnetic characteristics. In order to show the influence of different electromagnetic pulses on antenna coupling, a large number of repeated simulations is needed. Compared with the front-door coupling, the back-door coupling receives more concern. For example, there is a lot of theoretical and numerical research work on the shielding effectiveness of metal cavities with different forms of slots [10]. Mats Backstrom studied the field-to-wire coupling problem and regarded the wire as a receiving antenna [11]. As a full-wave electromagnetic algorithm in the time domain, FDTD is widely used to analyze the coupling between the electromagnetic pulse and the system. For the cable-coupling problem, the hybrid FDTD and transmission line method are usually used to analyze the coupling effect of transmission cables in different scenarios. In recent years, in order to analyze the electromagnetic coupling between cables and circuits, the SPICE model has been widely used because it can be used to simulate many circuit devices, such as transistors, capacitors, and inductors [12,13]. However, this method only establishes the SPICE model of the cable or lumped circuit and does not take into account the fact that the electronic system contains an antenna and cable in a real situation. That is, it does not take into account front-door coupling and back-door coupling together. In 2021, some scholars used the hybrid FDTD-SPICE method to analyze the coupling effect of wireless communication systems, including antennas, shielded cables, and metal-shielded cavities with slots under external EMP signals [14]. However, the SPICE model has its own defects: Dan Ren et al. found that the diode had reverse recovery and junction capacitance, which will produce high-order harmonic components at high frequencies, causing conducted interference and radiated interference, leading to electromagnetic compatibility problems. They extracted the diode model according to the measurement results and optimization algorithm, which is used to improve the traditional SPICE model [15]. Furthermore, the SPICE model cannot truly reflect the movement of internal carriers of semiconductor devices under the irradiation of the electromagnetic pulse and the electromagnetic characteristics displayed at the macro level; thus, it is necessary to introduce an improved equivalent circuit model based on a physical model.

Therefore, this paper takes the limiter as the target, introduces the improved equivalent circuit model based on the physical model, analyzes the influence of front-door and back-door joint coupling on its coupling power and limiting performance, and then puts forward protection suggestions for front-door and back-door coupling, respectively. Common measures to protect equipment from electromagnetic interference include electromagnetic shielding, grounding, and filtering. The specific actions include using non-metallic fiber-optic cables when possible and employing methods to decrease the resonance characteristics of critical equipment enclosures [16]. Frank Leferink has conducted a lot of work on electromagnetic interference and proposed lots of valuable advice, such as limiting the length of exposed cable and placing exposed cables out of the line of sight of transmitters above 400 MHz when common mode currents on cables are exposed to high-intensity radiated fields and a nuclear electromagnetic pulse [17].

The structure and main contribution of this paper are as follows. Section 2 introduces the SPICE model of the limiter and the improved equivalent circuit model based on the physical model. In Section 3, based on the improved equivalent circuit model, the joint-coupling characteristics of the front door and back door of the limiter are analyzed, and the protection suggestions of front-door limiting and back-door shielding are given. Section 4 is a summary. A flow chart illustrates the structure and main contributions of this paper in Figure 1.

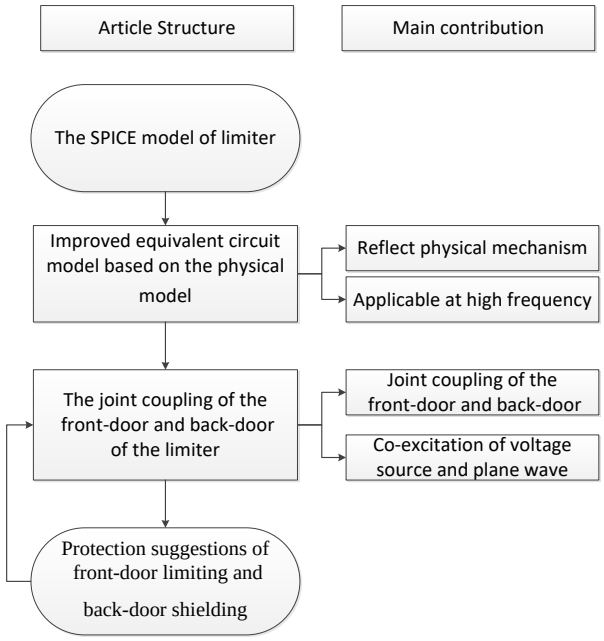

Figure 1. Flow chart for the structure and main contributions of this paper.

2. Theory and Model

This section first introduces the SPICE model of the limiter and gives the traditional equivalent circuit formula of the diode. Then, the diode simulation method based on the physical model, as well as the resulting improved equivalent circuit model, is described. Finally, we give the joint coupling scheme of the front-door and back-door of the limiter.

2.1. Traditional SPICE Model of Limiter

The common SPICE model of the single-stage and single-tube limiter is shown in Figure 2. R_A and R_L are equivalent line resistance and load impedance, both set to 50 Ω.

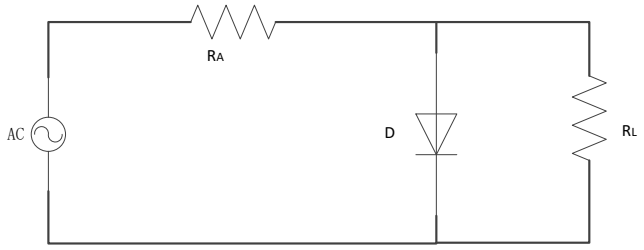

Figure 2. Single-stage and single-tube limiter.

As shown in Figure 3, the diode is located between nodes (i, j, k) and (i, j, k + 1). The current direction is the z direction, and I_d can be described by the following formula

$$I = I_d[e^{qV_d/kT} - 1] \quad (1)$$

where I_d is the dark current, q is the absolute value of electron charge, k is the Boltzmann constant, V_d is the voltage across the diode, and T is the thermodynamic temperature.

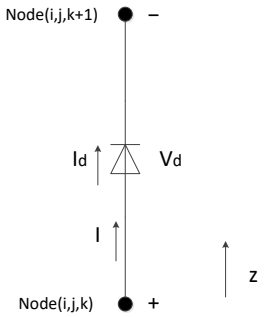

Figure 3. Schematic diagram of the diode.

2.2. Diode Formula Based on Physical Model

The traditional equivalent circuit formula cannot accurately reflect the device characteristics, especially in the case of high frequency, so the physical model is introduced. According to the theory of semiconductor devices, the basic equation consists of three parts: the carrier transport equation, continuity equation, and Poisson equation, which are summarized into a set of basic differential equations for the analysis of semiconductor devices:

$$\frac{\partial p}{\partial t} = -\frac{1}{q}\nabla \cdot \mathbf{J_p} + G_p - U_p \tag{2}$$

$$\frac{\partial n}{\partial t} = -\frac{1}{q}\nabla \cdot \mathbf{J}_n + G_n - U_n \tag{3}$$

$$\mathbf{J_p} = -qD_p\nabla p - q\mu_p p\nabla\psi \tag{4}$$

$$\mathbf{J_n} = -qD_n\nabla n - q\mu_n n\nabla\psi \tag{5}$$

$$\nabla\cdot\nabla\psi = -\frac{q}{\varepsilon}(N_d - N_a + p - n) \tag{6}$$

where ε, $\mathbf{J_n}$, ψ, $\mathbf{J_p}$, n, p, N_a, q, N_d, and t are the permittivity, electron current density, electrostatic potential, hole current density, electron concentrations, hole concentrations, hole doping concentrations, electronic charge, electron doping concentrations, and time, respectively. G_n and G_p represent carrier generation rates for the electron and hole. U_n and U_p are recombination rates for the electron and hole. D_p and D_n are the hole–diffusion coefficient and electron–diffusion coefficient.

According to the diode response curve fitted by the physical model, the improved equivalent circuit formula can be proposed [18]:

$$\begin{aligned} I = {} & \varepsilon(f_0 - f)\cdot I_0[e^{\frac{q}{kT}V_d} - 1] + \varepsilon(f - f_0)\Big\{\alpha\cdot\tfrac{1}{2\pi f L_0}V_d \\ & +\beta\cdot[\varepsilon(V_d - V_1)2\pi f C_1\cdot V_d + \varepsilon(V_1 - V_d)2\pi f C_2\cdot V_d]\Big\} \end{aligned} \tag{7}$$

where

$$\alpha = \frac{1}{1 + e^{a(V_d - V_0)}} \tag{8}$$

$$\beta = \frac{1}{1 + e^{-bV_d}} \tag{9}$$

where α and β are control coefficients, I represents the current flowing through the diode, I_0 represents the saturation current, q is the absolute value of the electron charge, k is the Boltzmann constant, and T is the thermodynamic temperature. V_d is the voltage across the diode, and V_0 is the empirical voltage value. f_0 is the empirical value; f represents the frequency of solving the problem; $\varepsilon(f_0 - f)$, $\varepsilon(f - f_0)$, $\varepsilon(V_d - V_1)$ and $\varepsilon(V_1 - V_d)$ represent the step function; L_0 is the empirical inductance value; C_1 and C_2 are empirical values; and V_1 represents the startup voltage of the diode.

The physical meaning of the formula is defined as follows: when the frequency f is lower than f_0, it is calculated according to the traditional empirical formula. When f is higher than f_0, the traditional empirical formula is no longer applicable. At high frequency and low voltage, the diode presents high impedance characteristics, and at high frequency and high voltage, the diode presents low impedance characteristics, and these are respectively used to control the diode response of low power input (equivalent to low input voltage) and high power input (equivalent to high input voltage) at high frequency.

2.3. Joint Analysis of Front-Door and Back-Door Couplings of PIN Limiter Based on Physical Model

In Sections 2.1 and 2.2, we introduce the limiter model based on the traditional equivalent circuit formula and the improved equivalent circuit formula based on the physical model. On this basis, we introduce how to create the front-door and back-door joint coupling of the limiter based on the physical model.

The system used in this paper consists of a receiving antenna and a limiter, which are placed in an equipment cabin with a slot, as shown in Figure 4. In order to study the influence of front-door and back-door coupling on the working characteristics of the limiter circuit, the following simplification is made: As introduced in the literature [14], there is an analytical relationship between the signal received by the antenna from the front door and the electromagnetic pulse, so the signal reaching the limiter can be expressed as a certain form of excitation source. This paper simplifies the front-door coupling through the antenna as the sine wave to the voltage source. The back-door coupling usually includes electromagnetic wave components from various frequencies in space, so the form of the plane wave adopts a Gaussian pulse. In order to maximize the effect of back-door coupling, a bare PIN circuit without any protective measures is adopted here. Here, we use both voltage source and plane wave excitation so as to simulate the joint coupling characteristics of the front door and back door under different electromagnetic pulses. Then, we give the protection scheme of front-door limiting and back-door shielding accordingly.

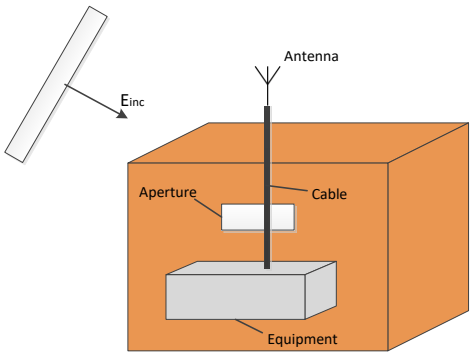

Figure 4. Typical wireless communication system illuminated by an electromagnetic pulse.

3. Numerical Simulation and Analysis

Based on the improved equivalent circuit formula extracted from the physical model proposed in the previous section, this section analyzes the joint coupling characteristics of the front door and back door of the limiter under the irradiation of the electromagnetic pulse and gives protection suggestions accordingly.

3.1. Simulation Effectiveness Verification

In order to verify the effectiveness of the simulation method, this section verifies the electromagnetic characteristics of the target under plane wave irradiation and voltage injection.

3.1.1. Front-Door Injection

The accuracy of the circuit response curve under voltage injection is verified below.

A. Traditional SPICE simulation

The response curve of the diode is obtained by the FDTD method, as shown in Figure 5, using the same simulation condition as reference [18]. When the source voltage is higher than 0.7 V, the sampling voltage of the diode remains at 0.7 V, which is consistent with the theoretical analysis [19].

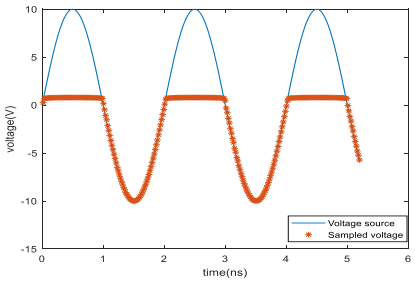

Figure 5. Diode response curve.

B. Improved equivalent circuit

Now, we start the simulation of the circuit shown in Figure 2 with the improved equivalent circuit formula. The voltage at both sides of the diode is observed. Here, we define f_0 = 2 GHz, V_0 = 10 V, L_0 = 6 H, a = 2, b = 2, C_1 = 100 pF, C_2 = 1 pF, and V_1 = 0.7 V. Three examples are given to verify the effectiveness of the improved equivalent circuit method.

- f = 400 MHz, V_m = 4 V

In the first example, we define the frequency of solving the problem as 400 MHz and the maximum amplitude of the excitation source as 4 V. It is used for testing the improved equivalent circuit formula under low frequency. The results are shown in Figure 6, which are consistent with the analysis in reference [18].

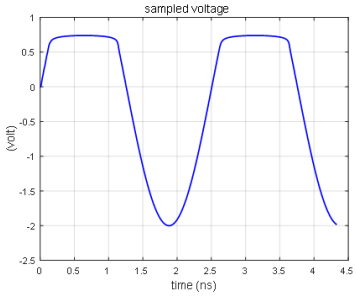

Figure 6. Result of improved equivalent circuit method under low frequency.

As we can see from the picture, it is consistent with the traditional equivalent circuit method.

- f = 4 GHz, V_m = 6 V

In the second example, we define the frequency of solving the problem as 4 GHz and the maximum amplitude of the excitation source as 6 V. It is used for testing the improved equivalent circuit formula under high-frequency and low-voltage injection. The results are shown in Figure 7, which are consistent with the analysis in reference [18].

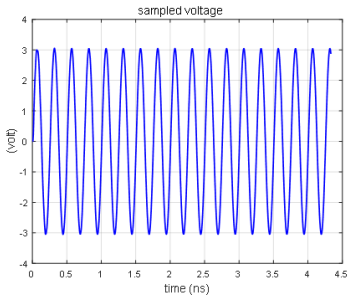

Figure 7. Result of improved equivalent circuit method under high-frequency and low-voltage injection.

The improved equivalent circuit method can feed back the characteristics similar to the physical model at high-frequency and low-voltage injection.

- f = 4 GHz, V_m = 30 V

In the third example, we define the frequency of solving the problem as 4 GHz and the maximum amplitude of the excitation source as 30 V. It is used for testing the improved equivalent circuit formula under high-frequency and high-voltage injection. The results are shown in Figure 8, which are consistent with the analysis in reference [18].

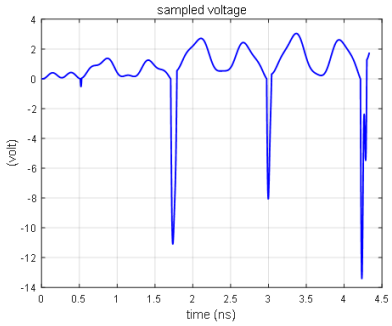

Figure 8. Result of improved equivalent circuit method under high-frequency and high-voltage injection.

As we can see from Figure 8, the improved equivalent circuit method can work at high frequency and high power.

3.1.2. Back-Door Irradiation

For testing the accuracy of the electromagnetic characteristics of the target under the plane wave irradiation, the plane wave is used to irradiate the dielectric sphere, the waveform of which is the Gaussian pulse. The propagation direction is the z direction, and the electric field direction is the x direction. The radius of the dielectric sphere is 10 cm, and the electromagnetic parameters are epsilon_r = 3, sigma_ e = 0.5 S/m, sigma_ m = 0.5 H/m, and mu_r = 2. The spatial step size is dx = dy = dz = 1 cm. We select the center position of the medium sphere as the reference point and obtain the comparison result with CST, as shown in Figure 9.

It can be seen that the FDTD simulation results compare well with CST, which proves the effectiveness of the FDTD algorithm in simulating the near-field coupling problem under plane wave irradiation.

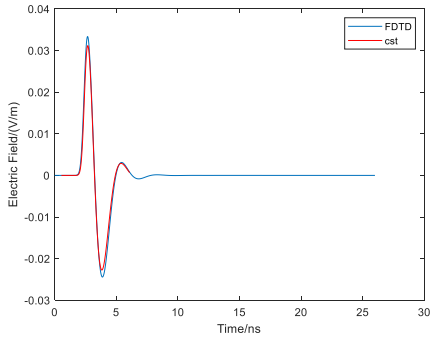

Figure 9. Comparison of field between FDTD and CST.

3.2. Joint Coupling Characteristics of Front Door and Back Door under Different Electromagnetic Pulse Irradiation

Based on Section 2.3, we start the process of joint analysis of front-door and back-door coupling. Firstly, no protective measures are taken for the front door and back door. The circuit used is shown in Figure 2. Because the limiter pays more attention to the output power, the final obvious target is the power on the load impedance. Under the same conditions, the voltage at both ends of the diode can be observed equivalently.

- Low-frequency condition

The voltage of the front-door coupling is mainly a low-frequency component, assuming that the frequency of the sine wave voltage is 400 MHz and the amplitude is 4 V. The amplitude of the Gaussian pulse of the back-door coupling is 1000 V/m, the propagation direction is along the z direction, and the electric field direction is the x direction. The mesh step is dx = dy = dz = 2 mm, and the model is shown in Figure 10. Setting the circuit size to 20 mm × 20 mm × 10 mm, we can observe the voltage at both ends of the diode and the field at the center.

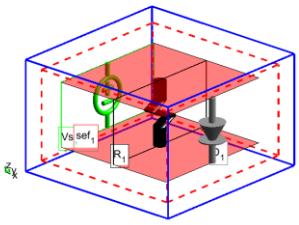

Figure 10. Model of single tube limiter.

The voltage at both ends of the diode is obtained by simulation.

In Figure 11, the influence of the applied Gaussian pulse on the voltage at both ends of the diode can be clearly seen, which makes the voltage–response curve different from that of front-door coupling only in Figure 6. We can see that a pulse whose absolute amplitude takes over 3 V has been introduced. In fact, this is a typical field-circuit coupling problem. As the diode in Figure 3 is located between the node (i, j, k) and the node (i, j, k + 1), the port voltage V_d can be deduced from the electric field path integral when there is no circuit excitation source:

$$V_d = \int_k^{k+1} \vec{E_d} \cdot dl \tag{10}$$

where E_d represents the coupling voltage caused by back-door coupling at both ends of the diode [20]. When the front-door and back-door coupling occurs at the same time, the voltage at both ends of the diode is the composition of the coupling voltage caused by back-door irradiation and the voltage caused by the excitation source injection of the front-door circuit. This explains the difference between the coupling voltage waveform at

both ends of the diode when the front door and rear door are coupled together and the coupling-voltage waveform when only the front door is injected.

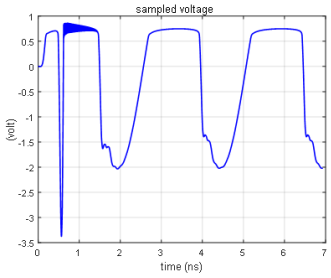

Figure 11. Voltage at both ends of diode at low frequency.

The dynamic changes of the electric field in the circuit are shown in Figure 12 below. These figures are all made by MATLAB 2018 using the animation function.

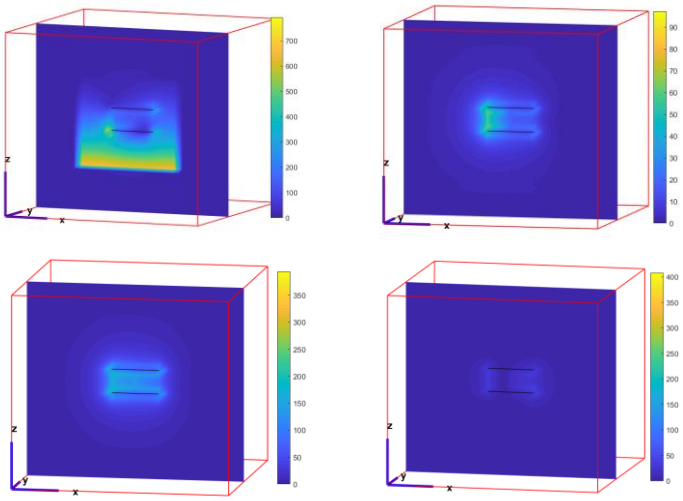

Figure 12. The dynamic changes of the electric field at low frequency.

- High-frequency condition

When the voltage of the front-door coupling is mainly a high-frequency component, it is assumed that the frequency of the sine wave is 4 GHz, the amplitude is 6 V, and the other settings are the same as those in low frequency before. The updated formula of the diode is in accordance with the improved equivalent circuit formula, and the voltage at both ends of the diode is simulated.

In Figure 13, the influence of the applied Gaussian pulse on the voltage at both ends of the diode can be clearly seen, which makes the voltage–response curve different from that of front-door coupling only in Figure 7. We can see that a pulse whose absolute amplitude takes over 5 V has been introduced. This can be explained as above. The dynamic changes of the electric field in the circuit are shown in the Figure 14 below.

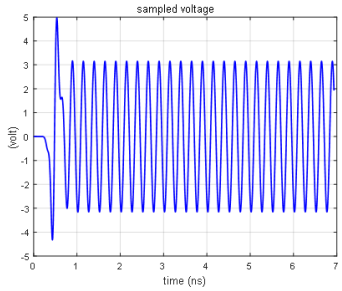

Figure 13. Voltage at both ends of diode at high frequency.

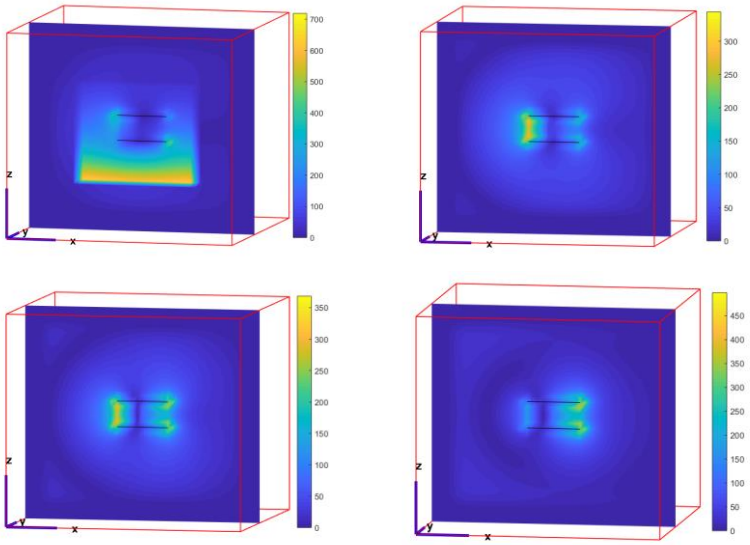

Figure 14. The dynamic changes of the electric field at high frequency.

3.3. Joint Coupling Characteristics of Front-Door and Back-Door Coupling after Taking Protection Measures

In order to reduce the electromagnetic coupling of the front door and back door, this paper adopts the protection scheme of front-door limiting and back-door shielding.

3.3.1. Single-Stage and Double-Tube Limiter

In order to achieve a better limiting effect of the front door, the single-tube limiter is changed to the double-tube, as shown in Figure 15.

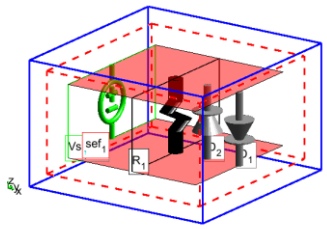

Figure 15. Double-tube limiter.

1. Low-frequency condition

The simulation setting is the same as when the frequency of the front-door coupling is 400 MHz, and the voltage at both ends of the diode is shown in Figure 16.

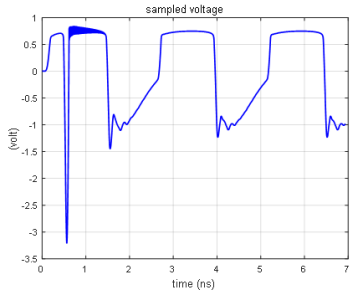

Figure 16. Voltage at both ends of the double-tube under low frequency.

Compared with Figure 11, it is found that the coupling voltage of the front door decreases significantly, which means that the output power decreases significantly. However, due to the lack of back-door protection, the back-door coupling voltage is still obvious. The dynamic changes of the electric field in the circuit are shown in the Figure 17 below.

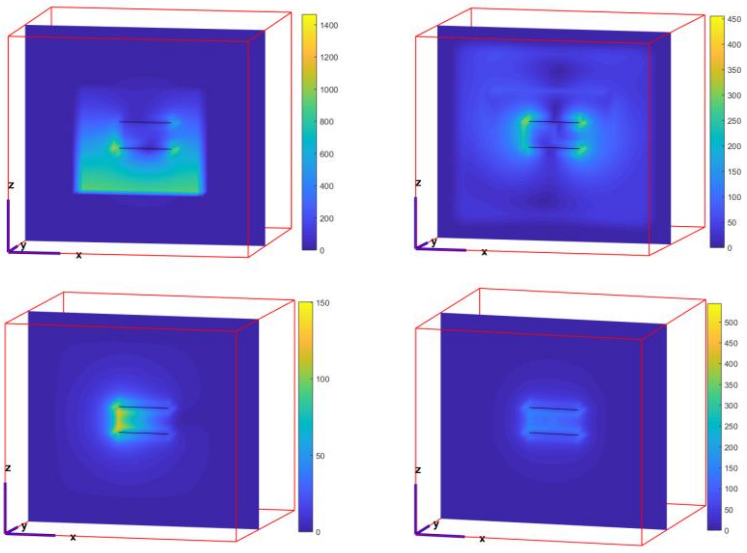

Figure 17. The dynamic changes of the electric field with double-tube under low frequency.

2. High-frequency condition

Setting the front-door coupling frequency to 4 GHz, the other settings are consistent with those at low frequency. The voltage at both ends of the diode of the double-tube limiter can be obtained in Figure 18.

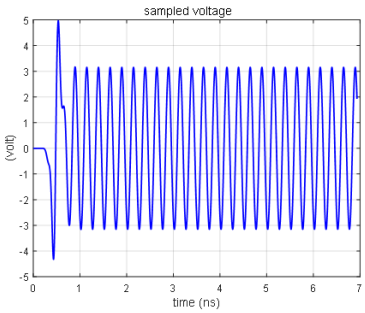

Figure 18. Voltage at both ends of double-tube under high frequency.

Compared with Figure 13, when the front door is injected with a high frequency and low voltage, the diode shows high impedance, which is equivalent to a large inductance. After the two tubes are connected in parallel, it is still a large inductance, so the coupling

waveform changes little compared with Figure 13. The dynamic changes of the electric field in the circuit are shown in the Figure 19 below.

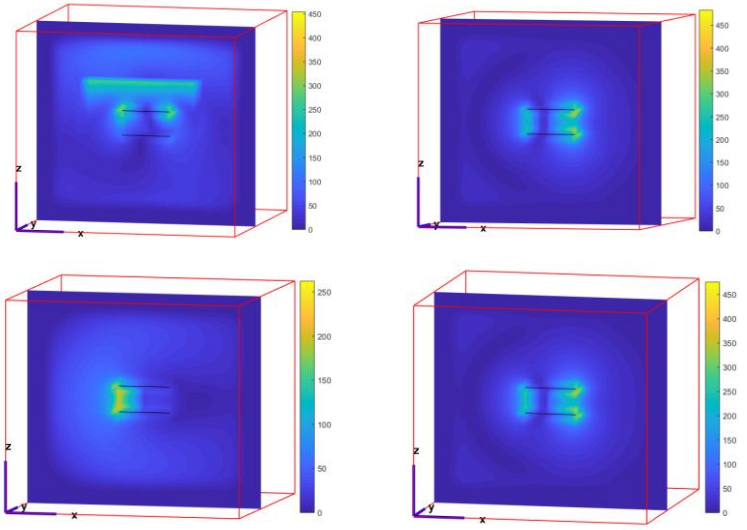

Figure 19. The dynamic changes of the electric field with double-tube under high frequency..

3.3.2. Limiter with Shielding Cavity

In order to reduce the influence of the back-door coupling on the performance of the limiter, the limiter is placed in a PEC metal shielding cavity. The size of the shielding cavity is 40 mm × 40 mm × 20 mm, and the wall thickness is 4 mm. In reality, it is difficult to achieve complete shielding, so a 4 mm × 4 mm × 4 mm hole is opened at the bottom of the shielding cavity to simulate this situation. The model is shown in Figure 20.

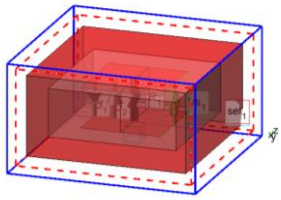

Figure 20. Shielding cavity with built-in limiter.

3. Low-frequency condition

The simulation setting is the same as that of the double-tube limiter at low frequency, and the voltage at both ends of the diode is obtained in Figure 21.

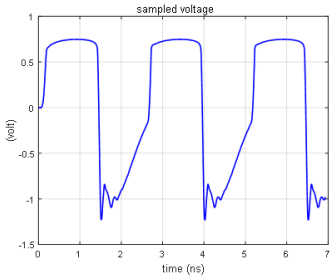

Figure 21. Voltage at both ends of diode with shielding cavity under low frequency.

Compared with Figure 16, it can be seen that due to the skin effect of the shielding cavity and the reflection of electromagnetic waves, the back-door coupling component has

been suppressed and eliminated, which proves the effectiveness of the shielding cavity. The dynamic changes of the electric field in the circuit are shown in the Figure 22 below.

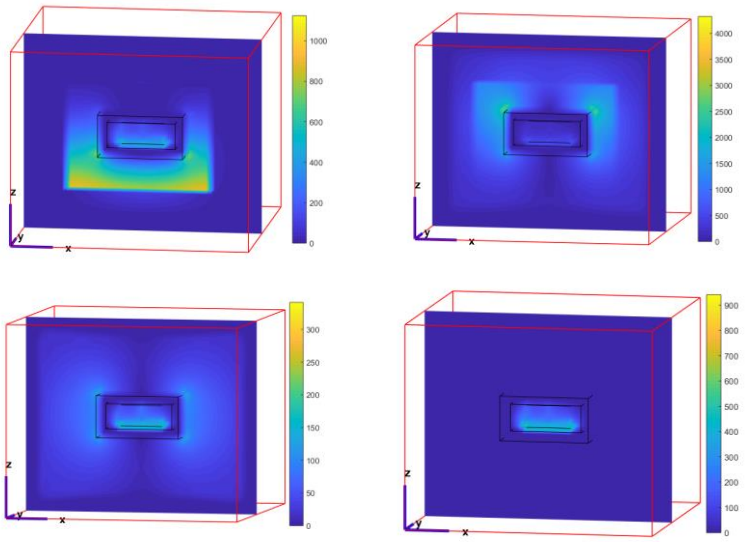

Figure 22. The dynamic changes of the electric field with shielding cavity under low frequency.

From the field calculation results, it is also clear that the back-door coupling is effectively suppressed due to the existence of the shielded cavity, which is consistent with the circuit analysis results.

4. High-frequency condition

The simulation setting is the same as that of the double-tube limiter at high frequency, and the voltage at both ends of the diode is obtained in Figure 23.

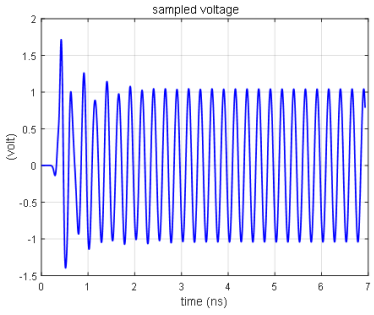

Figure 23. Voltage at both ends of the diode.

Compared with Figure 18, it can be seen that due to the skin effect of the shielding cavity and the reflection of electromagnetic waves, the back-door coupling component has been suppressed and eliminated, which proves the effectiveness of the shielding cavity. The dynamic changes of the electric field in the circuit are shown in the Figure 24 below.

From the field calculation results, it is also clear that the back-door coupling is effectively suppressed due to the existence of the shielded cavity, which is consistent with the circuit analysis results.

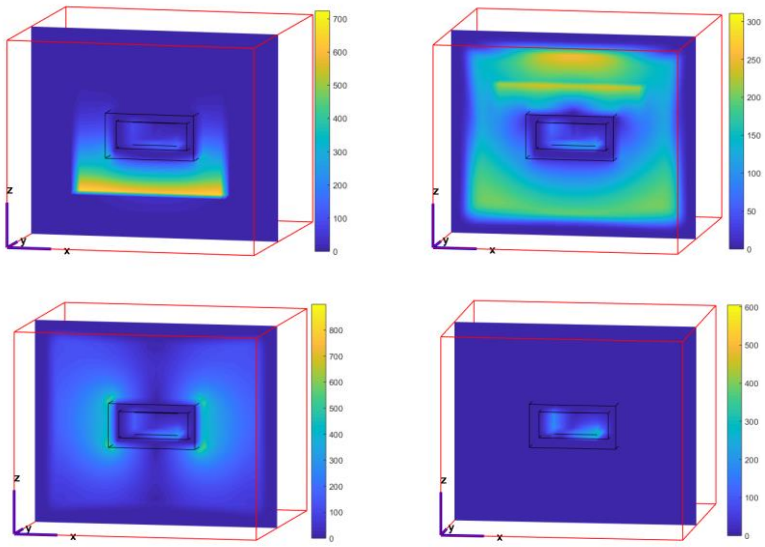

Figure 24. The dynamic changes of the electric field.

4. Conclusions

This paper studies the joint coupling effect of the front door and back door of the PIN limiter under electromagnetic pulse irradiation based on the physical model. Previous research on electromagnetic pulse coupling in electronic devices and systems focuses more on front-door or back-door coupling alone; thus, it cannot accurately reflect the situation when electronic devices and systems suffer from front-door and back-door coupling at the same time. More importantly, when front-door and back-door coupling occurs, the internal circuit is in a working state, and there is excitation. This factor should also be considered. In this paper, the front-door coupling is equivalent to the voltage injection, and the back-door coupling adopts the Gaussian pulse as the plane wave source in order to reflect the coupling of various frequency components to the system. This joint-coupling scheme of the front-door and back-door, with the voltage source and plane wave acting simultaneously, is rarely seen in previous analyses. In view of the limited application scenarios of the traditional equivalent circuit model, an improved diode equation based on the physical model is introduced. The improved equivalent circuit method can be used to analyze the working state of the diode circuit under large-injection and high-frequency conditions so as to expand its application scenarios. By adopting the scheme of "front-door limiting" and "back-door shielding", it is found that the voltage, finally coupled to both ends of the limiter diode, has been significantly reduced compared with that before the protection measures were taken. The equivalent understanding is that the power at both ends of the load has been significantly reduced. Therefore, it has obvious practical significance for protecting load devices.

Author Contributions: Conceptualization, B.Y.; methodology, L.X.; software, T.L.; validation, T.L.; formal analysis, T.L.; investigation, Q.L.; resources, L.X.; data curation, L.X.; writing—original draft preparation, T.L.; writing—review and editing, L.X.; visualization, T.L.; supervision, X.S.; project administration, X.S.; funding acquisition, Q.L. All authors have read and agreed to the published version of the manuscript.

Funding: This research was funded by the National Key Laboratory of Science and Technology on Space Microwave, grant number 6142411332211.

Data Availability Statement: Not applicable.

Conflicts of Interest: The authors declare no conflict of interest.

References

1. Liu, X.; Liu, Y.; Weng, X.; Lin, X.; Yang, Y. Fault Injection of Strong Magnetic Pulse in Digital Integrated Circuit. In Proceedings of the 2021 International Conference on Communications, Information System and Computer Engineering (CISCE 2021), Beijing, China, 14–16 May 2021; pp. 164–167.
2. Gutierrez, H.M.; Christoffersen, C.E.; Steer, M.B. An integrated environment for the simulation of electrical, thermal and electromagnetic interactions in high-performance integrated circuits. In Proceedings of the IEEE 8th Topical Meeting on Electrical Performance of Electronic Packaging (Cat. No.99TH8412), San Diego, CA, USA, 25–27 October 1999; pp. 217–220.
3. Huynh, H.A.; Jo, J.-M.; Nah, W.; Kim, S. EMC Qualification Methodology for Semicustom Digital Integrated Circuit Design. *IEEE Trans. Electromagn. Compat.* **2016**, *58*, 1629–1641. [CrossRef]
4. Becerra, J.; Lopez, Z.; Rangel, A.; Vega, F. A Comparison of Fitting Methods for Modeling the Front Door Coupling of Two Nearby Parabolic Antennas. In Proceedings of the 2018 USNC-URSI Radio Science Meeting (Joint with AP-S Symposium), San Diego, CA, USA, 8–13 July 2018; pp. 27–28.
5. Zhang, D.; Zhou, X.; Cheng, E.; Wan, H.; Chen, Y. Investigation on Effects of HPM Pulse on UAV's Datalink. *IEEE Trans. Electro. Compat.* **2020**, *62*, 829–839. [CrossRef]
6. Guo, L.; Xiao, L.; Chen, J.; Yang, M.; Yang, J. Electromagnetic Pulse Coupling Effect Analysis for Outboard Engine System of Vehicle. In Proceedings of the 2020 IEEE MTT-S International Microwave Workshop Series on Advanced Materials and Processes for RF and THz Applications (IMWS-AMP), Chongqing, China, 29–31 November 2021; pp. 1–3.
7. Omri, D.; Aguili, T. Time-domain techniques for electromagnetic coupling analysis of transient excitations of rectangular cavity through slot. *J. Electromagn. Waves Appl.* **2015**, *29*, 1297–1316. [CrossRef]
8. Hu, X.; Qiu, Y.; Xu, Q.; Tian, A.J. Transient Response of Microstrip Patch Antenna Loaded on a Vehicle Platform Illuminated by Electromagnetic Pulse. *Prog. Electromagn. Res. C* **2020**, *104*, 69–84. [CrossRef]
9. Sabath, F.; Nitsch, D.; Jung, M.; Weise, T.H. Weise, Design and setup of a short pulse simulator for susceptibility investigations. *IEEE Trans. Plasma Sci.* **2002**, *30*, 1722–1727. [CrossRef]
10. Konefal, T.; Dawson, J.; Marvin, A.; Robinson, M.; Porter, S. A Fast Circuit Model Description of the Shielding Effectiveness of a Box With Imperfect Gaskets or Apertures Covered by Thin Resistive Sheet Coatings. *IEEE Trans. Electromagn. Compat.* **2006**, *48*, 134–144. [CrossRef]
11. Silfverskiold, S.; Backstrom, M.; Loren, J. Microwave field-to-wire coupling measurements in anechoic and reverberation chambers. *IEEE Trans. Electromagn. Compat.* **2002**, *44*, 222–232. [CrossRef]
12. Fujita, K. MNL-FDTD/SPICE Method for Fast Analysis of Short-Gap ESD in Complex Systems. *IEEE Trans. Electromagn. Compat.* **2016**, *58*, 709–720. [CrossRef]
13. Wang, X.; Wang, L.; Zhuo, J.; Lu, X.; Yuan, M.; Zhou, J.; Liu, Q.H. A Hybrid CN-FDTD-SPICE Solver for Field-Circuit Analyses in Low-Frequency Wideband Problems. *IEEE Trans. Compon. Packag. Manuf. Technol.* **2020**, *10*, 1721–1728. [CrossRef]
14. Hu, X.; Qiu, Y.; Xu, Q.L.; Tian, J. A Hybrid FDTD–SPICE Method for Predicting the Coupling Response of Wireless Communication System. *IEEE Trans. Electromagn. Compat.* **2021**, *63*, 1530–1541. [CrossRef]
15. Ren, D.; Xu, G.; Li, J.-Q.; Pan, Z.-Y.; Zhao, X.; Du, P.-A. Improvement of the SPICE Model of Diode Based on Measurement and Nonlinear Fitting Random Optimization Algorithm. *Electronics* **2022**, *11*, 3461. [CrossRef]
16. IEEE. *IEEE Recommended Practice for Protecting Publicly Accessible Computer Systems from Intentional Electromagnetic Interference (IEMI), IEEE Std 1642-2015*; IEEE: Manhattan, NY, USA, 2015; pp. 1–39.
17. Leersum, B.; Ven, J.-K.; Bergsma, H.; Buesink, F.; Leferink, F. Protection Against Common Mode Currents on Cables Exposed to HIRF or NEMP. *IEEE Trans. Electro. Compat.* **2016**, *58*, 1297–1305. [CrossRef]
18. Liu, T.; Xu, L.; He, Y.; Wu, H.; Yang, Y.; Wu, N.; Yang, X.; Shi, X.; Wei, F. A Novel Simulation Method for Analyzing Diode Electrical Characteristics Based on Neural Networks. *Electronics* **2021**, *10*, 2337. [CrossRef]
19. Elsherbeni, A.; Demir, V. *The Finite Difference Time Domain Method for Electromagnetics: With MATLAB Simulations*; SciTech Publishing: New York, NY, USA, 2016.
20. Zeng, H.; Tang, Y.; Duan, X.; Chen, X. A Physical Model-Based FDTD Field-Circuit Co-Simulation Method for Schottky Diode Rectifiers. *IEEE Access* **2019**, *7*, 87265–87272. [CrossRef]